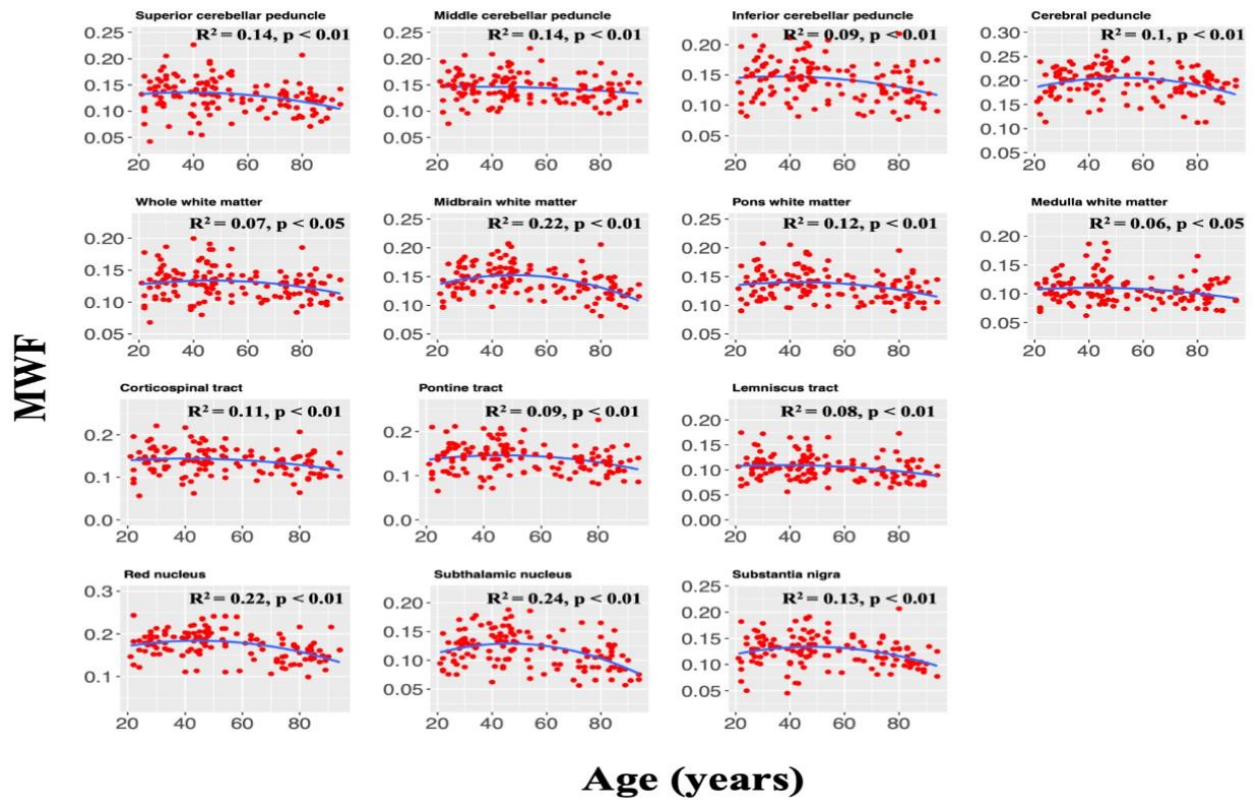
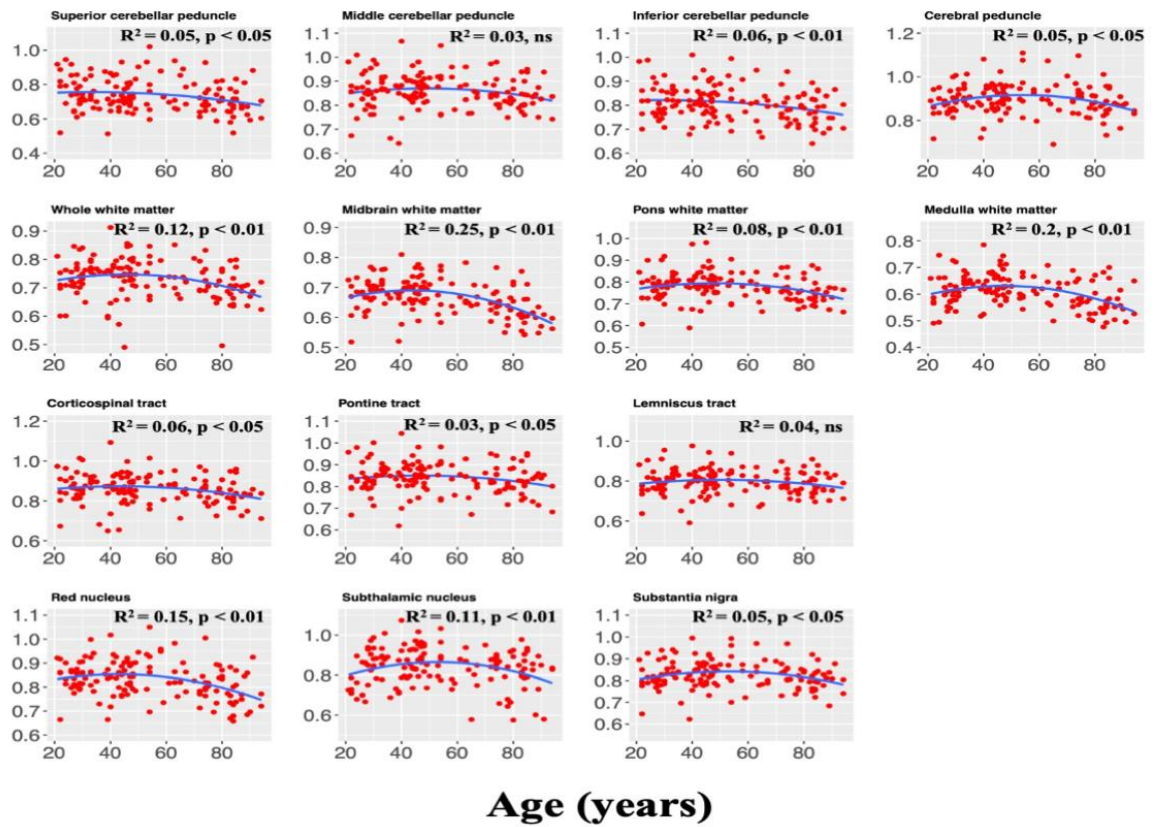


SUPPLEMENTARY FIGURES



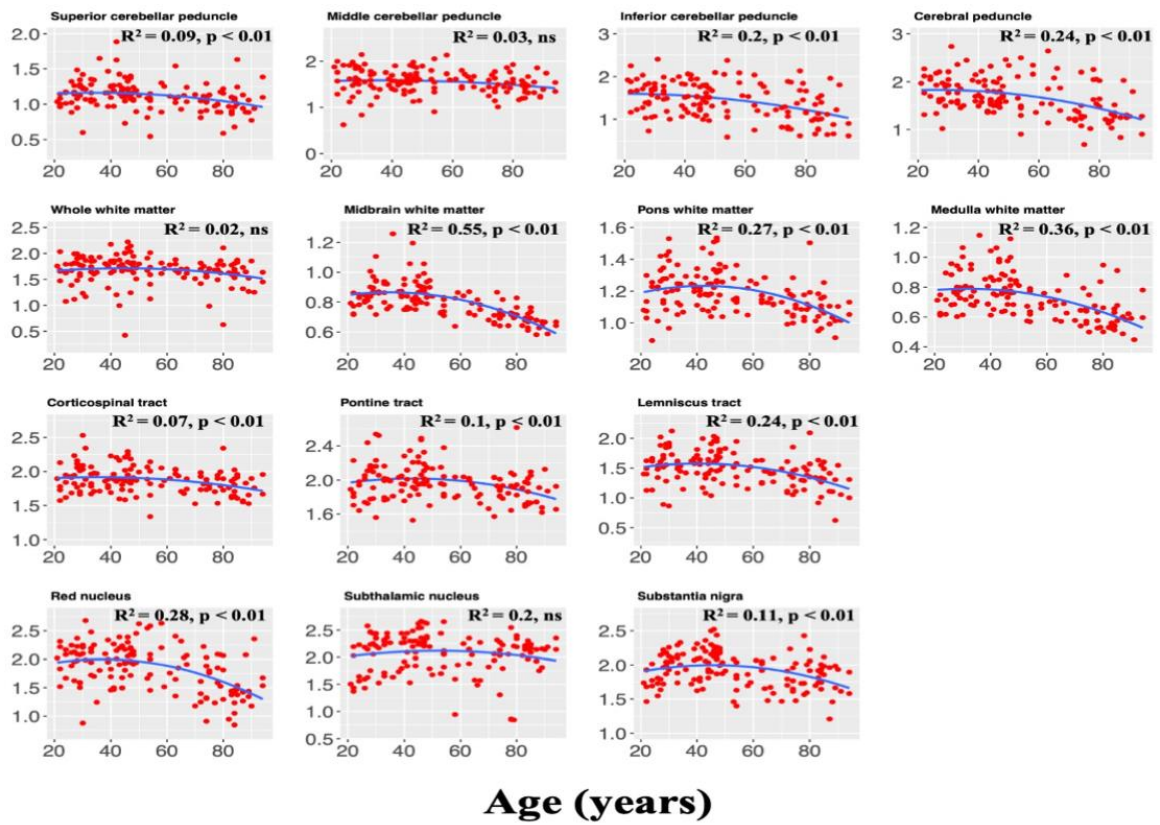
Supplementary Figure 1. Plots illustrating regional MWF values as a function of age white matter and deep grey nuclei substructures in the brainstem with a sample size of $N = 140$. For each ROI, the coefficient of determination, R^2 , and the significance of the linear regression model, p , are reported. Most regions investigated show an inverted U-shaped trend in MWF with age while exhibiting variation in these trends.

R_1 ($10^{-3} \times \text{ms}^{-1}$)

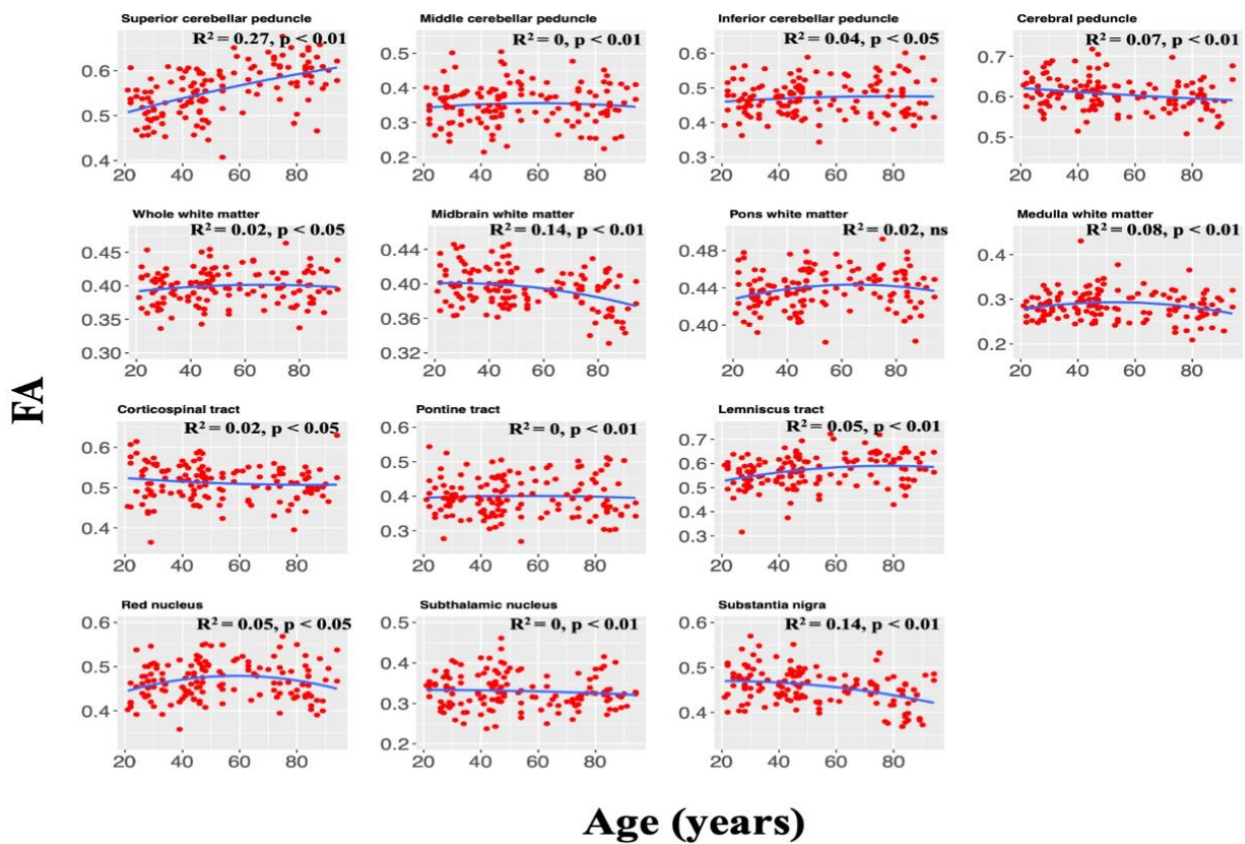


Supplementary Figure 2. Plots illustrating regional R_1 values as a function of age for white matter and deep grey nuclei substructures in the brainstem with a sample size of $N = 140$. For each ROI, the coefficient of determination, R^2 , and the significance of the linear regression model, p , are reported. All regions investigated show an inverted U-shaped trend in R_1 with age while exhibiting variation in these trends.

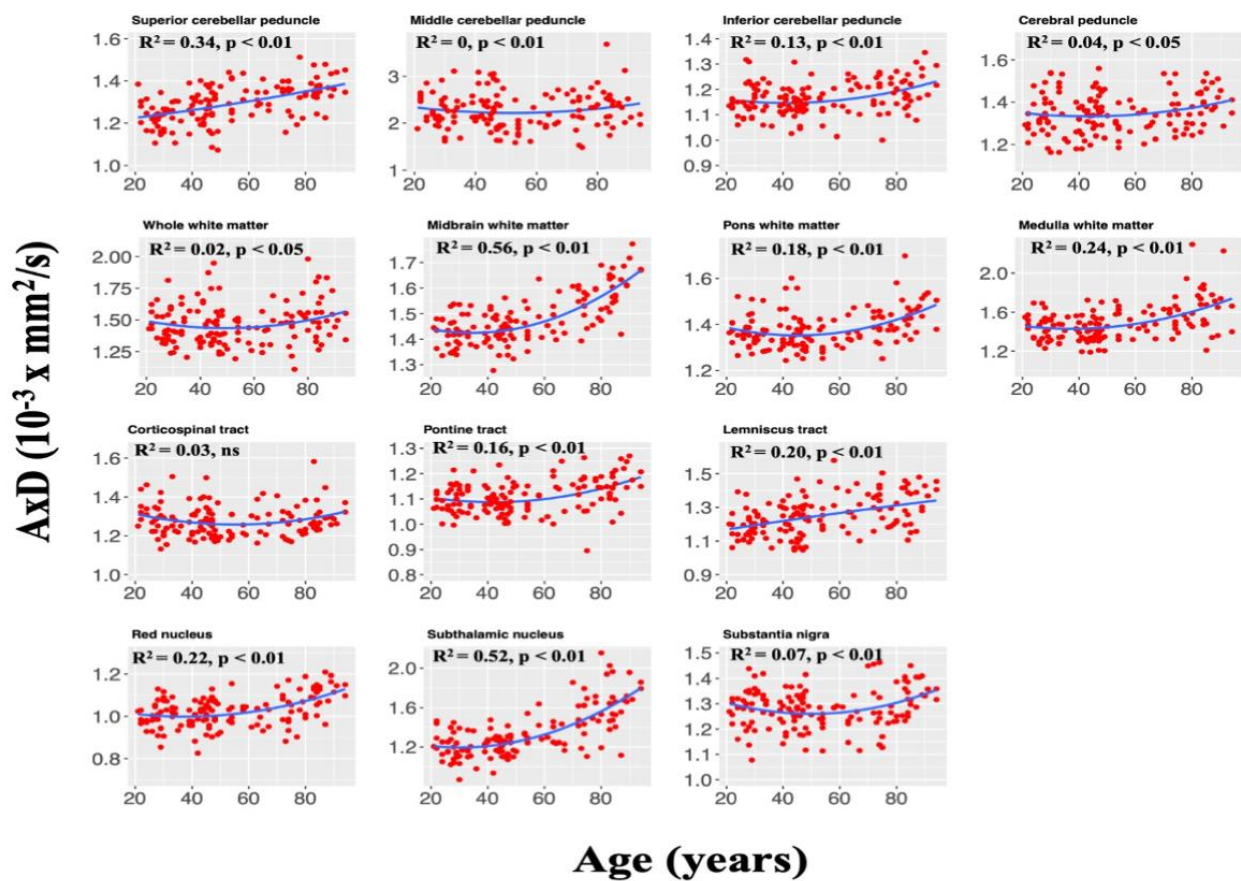
R_2 ($10^{-3} \times \text{ms}^{-1}$)



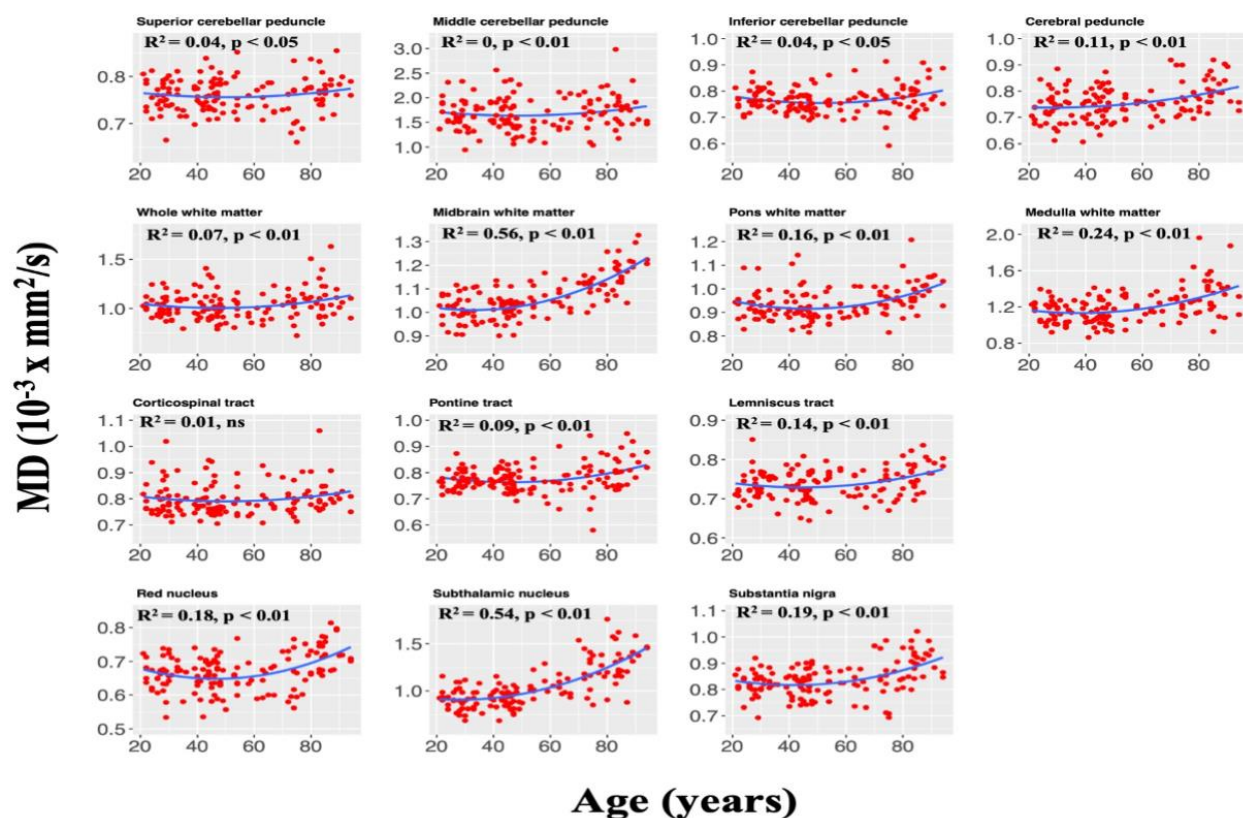
Supplementary Figure 3. Plots illustrating regional R_2 values as a function of age for white matter and deep grey nuclei substructures in the brainstem with a sample size of $N = 140$. For each ROI, the coefficient of determination, R^2 , and the significance of the linear regression model, p , are reported. All regions investigated show an inverted U-shaped trend in R_2 with age while exhibiting variation in these trends.



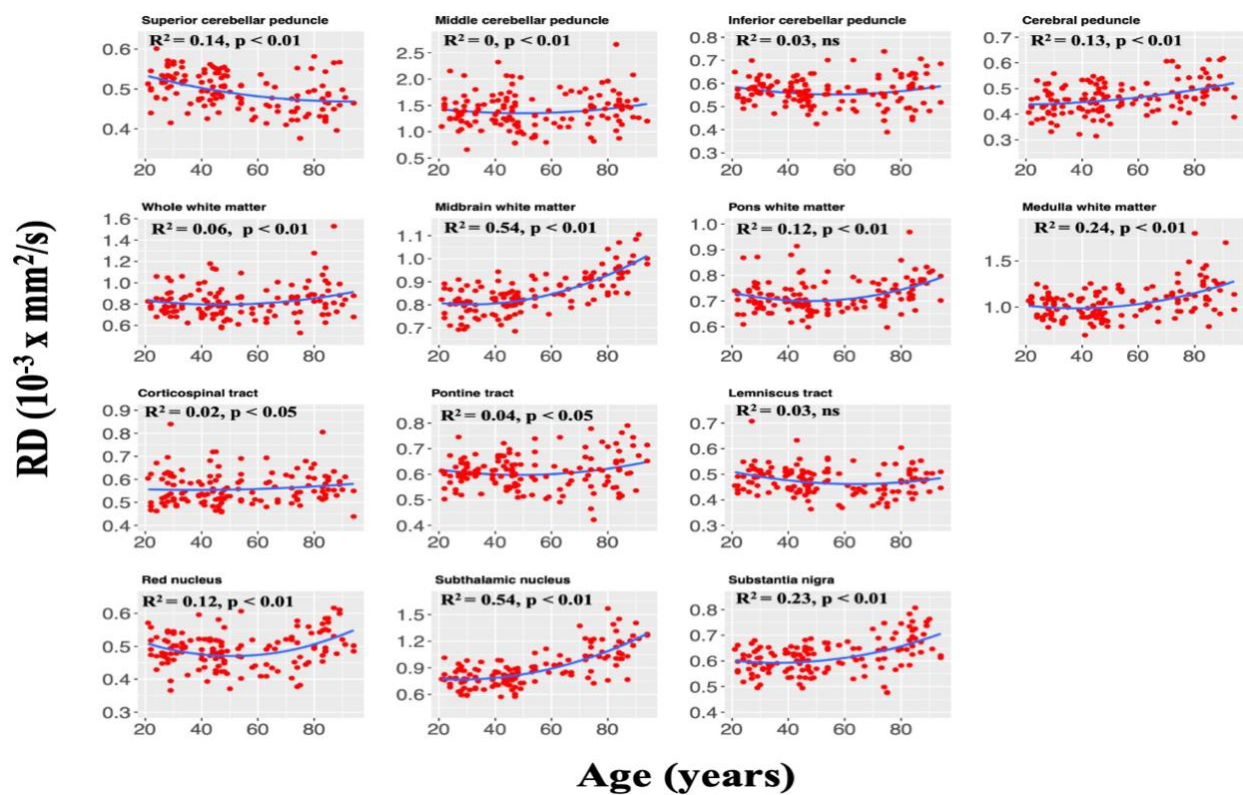
Supplementary Figure 4. Plots illustrating regional FA values as a function of age for white matter and deep grey nuclei substructures in the brainstem with a sample size of $N = 137$. For each ROI, the coefficient of determination, R^2 , and the significance of the linear regression model, p , are reported. The red nucleus, whole WM midbrain WM, pons WM, medulla WM, substantia nigra, and lemniscus tract exhibited a quadratic trend of age with FA. The cerebral peduncle and superior cerebellar peduncle showed a linear trend of FA with age while the remaining regions did not show a significant association between FA and age.



Supplementary Figure 5. Plots illustrating regional AD values as a function of age for white matter and deep grey nuclei substructures in the brainstem with a sample size of $N = 137$. For each ROI, the coefficient of determination, R^2 , and the significance of the linear regression model, p , are reported. A majority of the regions investigated show a U-shaped trend of AxD with age while exhibiting variation in these trends.



Supplementary Figure 6. Plots illustrating regional MD values as a function of age for white matter and deep grey nuclei substructures in the brainstem with a sample size of $N = 137$. For each ROI, the coefficient of determination, R^2 , and the significance of the linear regression model, p , are reported. A majority of the regions investigated show a U-shaped trend of MD with age while exhibiting variation in trends.



Supplementary Figure 7. Plots illustrating regional RD values as a function of age for white matter and deep grey nuclei substructures in the brainstem with a sample size of $N = 137$. For each ROI, the coefficient of determination, R^2 , and the significance of the linear regression model, p , are reported. A majority of the regions investigated show a U-shaped trend of RD with age while exhibiting variation in trends.